This article has been accepted for publication in a future issue of this journal, but has not been fully edited. Content may change prior to final publication. Citation information: DOI 10.1109/TSG.2020.3017952, IEEE Transactions on Smart Grid

Optimal DG Allocation and Volt−var Dispatch for a Droop Based Microgrid

Yusuf Gupta, *Student Member, IEEE,* Suryanarayana Doolla, *Senior Member, IEEE*, Kishore Chatterjee, *Member, IEEE* and Bikash Chandra Pal, *Fellow, IEEE*

***Abstract*— Unequal reactive power sharing amongst distributed generators (DG) is a significant concern while operating a droop based microgrid. The reasons for this unequal reactive power sharing include the difference in feeder impedances, uneven distribution of loads and DGs in terms of size and locations. In this paper, a mixed-integer linear programming (MILP) problem applicable for a droop based microgrid has been proposed to achieve proportional reactive power sharing amongst DGs while maintaining very low line losses. Firstly, the optimal sizing and placement of DGs are investigated. This includes a detailed discussion on the linearisation of various nonlinear terms involved in the formulation. Subsequently, a day−ahead dispatch is generated for these DGs for a given load profile. Additionally, network reconfiguration has been incorporated for further improvement in performance. The effect of considering a practical constant impedance-current-power (ZIP) load model, instead of simply considering constant impedance loads, has also been assessed. The proposed formulation has been tested on a 33 bus network which has been modified to represent an islanded microgrid. The results obtained validate the accuracy of the proposed planning and dispatch method and demonstrate its utility in achieving proportional reactive power sharing amongst the DGs while incurring very low line losses.**

***Index Terms*— Droop control, microgrid, loss minimisation, MILP optimisation, reactive power sharing, reconfiguration, sizing siting, volt−var.**

I. Introduction

The electric grid all over the world is being transformed by decreasing fossil-fuel based power generation and increasing renewable-based generation. It has led to increased penetration of distributed generators (DG) into the grid, especially at the distribution voltage level [1]. Such active distribution networks can also be operated as microgrids. Microgrids can operate in grid-connected mode and also in autonomous mode during grid or weather contingencies.

A hierarchical architecture is gaining popularity for executing the control and optimisation functions for a microgrid [2]. The lowermost level, which serves as the primary control is responsible for maintaining the voltage and for sharing power amongst the DGs. Primary control is desired to operate without employing communication for increased reliability and to have plug-n-play feature. Secondary control which operates on a slower time scale is generally responsible for voltage and frequency restoration. Tertiary layer, which is the outermost control layer, takes care of the optimal operation of the microgrid, and it also exchanges data with the electricity market layer.

In the islanded mode of operation, the main goal of the DGs is to collectively supply power to the loads within the network. The DGs are expected to share both active and reactive power in proportion to their ratings. Proportional power sharing amongst DGs is usually implemented by using droop control. It is well known that proportional active power sharing can easily be achieved by using conventional droop control. However, achieving proportional reactive power sharing is difficult due to differences in line impedances, uneven load distribution and suboptimal allocation (sizing and placement) of DGs across the network [3]. However, if proportional reactive power sharing is not implemented properly, then there are high chances of smaller DGs hitting their current limits because of higher reactive power output from them. These DGs would trip for the sake of their protection once their current limit is hit. This, in turn, would lower the overall generation capacity in the microgrid. This, in effect, may cause overloading and tripping of DGs which are remaining in the network because they now have to supply more power. Hence, a partial or complete shut down of the microgrid may happen. To avoid such scenarios, it is important to implement proportional reactive power sharing for avoiding overload of DGs.

The reactive power flow and its proportional sharing also get altered whenever there is a change in load, or a change in the network structure/topology, e.g., due to network reconfiguration. The issue of reactive power sharing has been explored in the literature extensively. The methods present in the literature can be roughly classified into two categories, *viz.*, those involving novel control strategies [3]–[15] and those involving novel optimisation routines [16]–[21]. The control strategies can be further grouped into one of the following three approaches; either adjusting the $Q-V$ droop coefficients (n_q) [5], [7] or the nominal voltages (V_n)

Y. Gupta and S. Doolla are with the Department of Energy Science and Engineering, and K. Chatterjee is with the Department of Electrical Engineering, Indian Institute of Technology Bombay, Mumbai 400076, India.

B.C. Pal is with the Control and Power Research Group, Electrical and Electronic Engineering Department, Imperial College London, London SW7 2AZ, U.K.

1949-3053 (c) 2020 IEEE. Personal use is permitted, but republication/redistribution requires IEEE permission. See http://www.ieee.org/publications_standards/publications/rights/index.html for more information.
Authorized licensed use limited to: Imperial College London. Downloaded on August 29,2020 at 19:16:47 UTC from IEEE Xplore. Restrictions apply.

This article has been accepted for publication in a future issue of this journal, but has not been fully edited. Content may change prior to final publication. Citation information: DOI 10.1109/TSG.2020.3017952, IEEE Transactions on Smart Grid

[4], [6], [12] or the virtual impedances (Z_v) [8], [11], [14]. Many of these control strategies, such as those employing distributed secondary controllers can achieve accurate reactive power sharing [11]–[13], [15], [22]. However, these control strategies do not explicitly take voltage and current limits of the remote nodes/branches into account. Hence, for a reasonably large and complex network, there are high chances of voltage violations at remote nodes, which can also affect voltage-sensitive loads. These aspects can be handled using central control architecture effectively.

The reactive power sharing problem has also been investigated by the use of optimisation algorithms. For example, reactive power sharing can be improved by optimising n_q [17], [18], V_n [20] and Z_v [16], [19]. Optimal $Q-V$ droop slope has been calculated in [17] for all the DGs for achieving equal reactive power sharing; however, the resultant active power sharing gets disturbed. Besides, the method has been tested for PQ loads only. A particle swarm optimisation (PSO) algorithm has been applied to calculate optimal Z_v in [16]. However, the obtained reactive power sharing is not proportional, and only constant impedance load have been investigated. PSO has also been applied in [18] to find optimal V_n for minimising the reactive power sharing error. A genetic algorithm has been applied to optimise Z_v for improving reactive power sharing in [19]. A multi-objective optimisation has been proposed in [20] for voltage regulation and reactive power distribution amongst DGs. Authors in [21] have designed a nonlinear droop curve for minimising operating cost and improving reactive power sharing using PSO.

The size and locations of the DGs affect the reactive power sharing, line losses and the voltage profile simultaneously [10], [18]. Arbitrary planning of DGs worsens the aforementioned parameters. Hence, the size and location of the DGs should be planned judiciously. The sizing and placement of DGs have been widely investigated for different technical and economic objectives for active distribution networks and grid-tied microgrids [23]. The size and the location of the DGs are usually decided at the planning stage based on objectives such as installation/operation cost minimisation [24], [25], line loss minimisation [26], demand reduction [27] and load curtailment [28]. To the best of authors' knowledge, reference [29] is the only work related to sizing of DGs for a droop-based islanded microgrid. In this work, authors have optimised the droop slopes of the DGs to minimise fuel consumption, to improve the voltage stability and the voltage profile of the microgrid. However, the optimal placement of the DGs is not investigated. Also, the obtained droop slopes are unrealistic and are unsuitable for a stable operation of the microgrid. Besides, even the basic active power sharing has not been achieved. Please note that an optimisation formulation for droop based microgrid is discussed in [30]. However, this work is applicable only for dispatch and does not perform DG allocation. Hence, there exists a need for a novel formulation for islanded droop-based microgrids which can be used for both DG allocation (optimal sizing and siting) and dispatch.

It is well known that the reactive power sharing and the network power loss is tightly linked with the voltage at different buses. Hence, n_q of all the DGs can be optimised for minimising real power loss [31] along with improving reactive power sharing. It is also well known that network reconfiguration along with volt-var control can substantially improve the voltage profile, reduce the line losses [32], improve the voltage stability, and loadability [30]. Coordinated volt-var control of DGs and scheduling of network reconfiguration switches can provide additional flexibility for reactive power control. They can also result in improved performance during both the planning and operation stages.

To the best of the authors' knowledge, none of the DG allocation studies for setting up microgrids have considered reactive power sharing as an objective which is crucial for avoiding overload of smaller DGs. Besides, none of the work related to either control strategy or optimisation has explored network reconfiguration to improve reactive power sharing. Besides, none of the work related to reactive power sharing has taken the constant impedance-current-power (ZIP) model into account, which also affects the reactive power flow. Motivated by the aforementioned observations, optimal allocation and volt−var dispatch of DGs and reconfiguration switches for a droop based microgrids have been proposed in this paper for achieving proportional reactive power sharing along with very low line losses.

The novelty and the contribution of this work as compared to the available literature is as follows.

- A mixed-integer linear programming (MILP) problem for DG allocation and dispatch has been proposed, including a detailed discussion on the linearisation process. To the best of authors' knowledge, the presented work is the first attempt to formulate an optimal DG sizing *and* placement problem for a *droop-based* microgrid.
- The optimal sizing and placement of DGs have been performed for achieving accurate reactive power sharing while ensuring near-optimal line losses.
- Network reconfiguration has been proposed and investigated as an additional degree of freedom for controlling the reactive power sharing.
- It is shown that the same formulation (with a few simplifications) can be used for DG allocation and optimal day-ahead dispatch.

The paper is organised as follows. The proposed MILP formulation is presented in Section II. The validation of the proposed method of allocation and dispatch, along with other case studies, is presented in Section III. Finally, Section IV contains the conclusion.

1949-3053 (c) 2020 IEEE. Personal use is permitted, but republication/redistribution requires IEEE permission. See http://www.ieee.org/publications_standards/publications/rights/index.html for more information.
Authorized licensed use limited to: Imperial College London. Downloaded on August 29,2020 at 19:16:47 UTC from IEEE Xplore. Restrictions apply.

This article has been accepted for publication in a future issue of this journal, but has not been fully edited. Content may change prior to final publication. Citation information: DOI 10.1109/TSG.2020.3017952, IEEE Transactions on Smart Grid

II. Proposed MILP Formulation

This section contains a detailed description of the proposed MILP formulation. The optimisation objective, the constraints and limits are explained step-by-step.

The primary control layer of the hierarchical control architecture is responsible for power sharing amongst the DGs. The well-known droop control is implemented in each DG for achieving proportional power sharing:

$$\omega_s = \omega_n - m_{p.s.i} P_{s.i} \tag{1}$$

$$V^{re}_{s.i} = V_{n.s.i} - n_{q.s.i} Q_{s.i} \tag{2}$$

where ω_n is the rated frequency in rad/s. ω_s, $m_{p.s.i}$ and $n_{q.s.i}$ are the reference frequency, $P-\omega$ droop slope and $Q-V$ droop slope of the s^{th} DG placed at the i^{th} bus. $P_{s.i}$ and $Q_{s.i}$ are the calculated active and reactive power output of the DG. $V_{n.s.i}$ and $V^{re}_{s.i}$ are the rated value and the reference value of the peak of the phase voltage of the DG.

m_p and n_q values are set in inverse proportion to the rating of the respective DG to achieve proportional power sharing. It is well known that the $P-\omega$ droop assists in achieving proportional active power sharing since the frequency is the same across the microgrid. Hence, achieving $m_{p1}P_1 = m_{p2}P_2 = ... = m_{pn}P_n$ is possible. However, the reactive power sharing is not proportional because the voltage is different for each DG. The primary reason for different voltages is the asymmetry in sizes and location of loads, non-uniform lengths of the feeders and asymmetry in location and size of the DG itself. This makes achieving $n_{q1}Q_1 = n_{q2}Q_2 = ... = n_{qn}Q_n$ difficult. Thus, optimal placement and sizing of DGs can significantly improve reactive power sharing amongst them. Hence, the optimisation objective is to minimise the reactive power sharing error for all the DGs simultaneously.

A. Objective function

The optimisation objective is to minimise the error between the expected reactive power output and the actual reactive power output of all the DGs. Perfect proportional reactive power sharing can be achieved by aiming for $n_{q.1}Q_1 = n_{q.2}Q_2 = ... = n_{q.s}Q_s$. As observed from (2), the n_qQ terms represent droop-induced voltage deviations ($V_{n.s} - V^{re}_s$). Let these terms be denoted by δV^q_s. Hence, the aim of the optimisation translates to minimising the difference between the δV^q_s terms of all the DGs. Thus, the objective function is formulated as follows:

$$min. \sum \Delta V^q_{s.i.j} \tag{3}$$

where i and j denote different buses of the microgrid. The range for both i and j is from one till N_b, wherein N_b is the total number of buses in the network. $\Delta V^q_{s.i.j}$ is calculated for every combination of i and j since a DG may or may not get placed at all the considered combinations of i and j. In effect, $\sum \Delta V^q_{s.i.j}$ would be a scalar quantity consisting of the sum of $N_b \times N_b$ terms. For example, for a 33 bus microgrid, $\sum \Delta V^q_{s.i.j}$ would contain the sum of 33*33 terms starting from $\Delta V^q_{s.1.1}$, $\Delta V^q_{s.1.2}$, $\Delta V^q_{s.1.3}$ till $\Delta V^q_{s.33.33}$.

$\Delta V^q_{s.i.j}$ is defined as follows:

$$\Delta V^q_{s.i.j} \geq \delta V^q_{s.i} - \delta V^q_{s.j} + V^q_\epsilon \tag{4}$$

The lower limit for $\Delta V^q_{s.i.j}$ is set as follows to ensure that only absolute values of $\Delta V^q_{s.i.j}$ are considered:

$$\Delta V^q_{s.i.j} \geq 0 \tag{5}$$

A correction term V^q_ϵ has been introduced in (4) because it is not known beforehand, whether DGs would get placed at both the buses i and j. V^q_ϵ needs to be set precisely equal to zero if the DGs get placed at both the buses i and j. The following two inequalities are applied to implement this condition.

$$V^q_\epsilon \geq (\lambda_{s.i} + \lambda_{s.j} - 2)(V_{max} - V_{min}) \tag{6}$$

$$V^q_\epsilon \leq 0 \tag{7}$$

Here, λ_s is a binary variable representing the presence of a DG at a particular bus. $\lambda_{s.i} = 1$ indicates the presence of a DG at a bus i and $\lambda_{s.i} = 0$ would indicate otherwise. Also, V_{min} and V_{max} correspond to the minimum and maximum magnitude allowed for the phase voltage throughout the microgrid.

Now, for $\lambda_{s.i} = 1$ and $\lambda_{s.j} = 1$, $V^q_\epsilon \geq 0$ because of (6) and $V^q_\epsilon \leq 0$ because of (7), thus ensuring $V^q_\epsilon = 0$. Consequently, $V^q_\epsilon = 0$ in combination with (5) transforms (4) to $\Delta V^q_{s.i.j} = \delta V^q_{s.i} - \delta V^q_{s.j}$.

On the other hand, it is desired that $\Delta V^q_{s.i.j}$ should be set precisely to zero when a DG is not placed at either i or j or both. The scenario for one of these three combinations is explained as follows. Consider $\lambda_{s.i} = 0$ and $\lambda_{s.j} = 0$. Theoretically, $\delta V^q_{s.i} - \delta V^q_{s.j}$ can take a maximum value of $2(V_{max} - V_{min})$. In such a condition, V^q_ϵ should be allowed to take a value equal to $-2(V_{max} - V_{min})$ to render a zero value for the right-hand side of (4). This is implemented with the help (6). Thus, $\Delta V^q_{s.i.j}$ would be forced to go to zero.

B. Constraints, linearisation, and limits

This subsection contains all the equality and inequality constraints as well as the limits applied to all the variables. It also contains the steps taken in linearising the nonlinear equations/terms.

1) KCL equations: The KCL equations for the i^{th} bus can be written in the Cartesian coordinates as follows:

$$I^{re}_{s.i} + I^{re}_{fi-i} = I^{re}_{l-i} + I^{re}_{fo-i} \tag{8}$$

$$I^{im}_{s.i} + I^{im}_{fi-i} = I^{im}_{l-i} + I^{im}_{fo-i} \tag{9}$$

where $I_{s.i}$ is the current supplied by the DG present at the bus i, I_{fi-i} is the line current flowing towards the bus i,

1949-3053 (c) 2020 IEEE. Personal use is permitted, but republication/redistribution requires IEEE permission. See http://www.ieee.org/publications_standards/publications/rights/index.html for more information.
Authorized licensed use limited to: Imperial College London. Downloaded on August 29,2020 at 19:16:47 UTC from IEEE Xplore. Restrictions apply.

This article has been accepted for publication in a future issue of this journal, but has not been fully edited. Content may change prior to final publication. Citation information: DOI 10.1109/TSG.2020.3017952, IEEE Transactions on Smart Grid

I_{l-i} is the load current and I_{fo-i} is the line current flowing away from the bus. Superscripts re and im denote the real and imaginary parts, respectively. The branch current I_{ij} is constrained as follows:

$$-I_{max}^{re} \leq I_{ij}^{re} \leq I_{max}^{re} \tag{10}$$

$$-I_{max}^{im} \leq I_{ij}^{im} \leq I_{max}^{im} \tag{11}$$

where I_{max}^{re} and I_{max}^{im} are determined as follows.

$$I_{max}^{re} = \frac{P_s^{max}}{1.5\ V_{min}} \tag{12}$$

$$I_{max}^{im} = \frac{Q_s^{max}}{1.5\ V_{min}} \tag{13}$$

where P_s^{max} and Q_s^{max} are the upper limits for $P_{s.i}$ and $Q_{s.i}$ respectively.

2) KVL equations: The KVL equations for the branch connecting the bus i and j is written as follows:

$$V_i^{re} = V_j^{re} + R_{ij}I_{ij}^{re} - X_{ij}I_{ij}^{im} \tag{14}$$

$$V_i^{im} = V_j^{im} + X_{ij}I_{ij}^{re} + R_{ij}I_{ij}^{im} \tag{15}$$

where V_i and V_j represent the phase voltage at bus i and j respectively. R_{ij} and X_{ij} are the resistance and reactance of the branch connecting bus i to j. The magnitude of the bus voltage can be expressed as follows:

$$V_i = \sqrt{(V_i^{re})^2 + (V_i^{im})^2} \tag{16}$$

Further, V_i is limited as follows:

$$V_{min}^2 \leq (V_i^{re})^2 + (V_i^{in})^2 \leq V_{max}^2 \tag{17}$$

The maximum and minimum phase angles allowed for the voltage phasor are represented by θ_{max} and θ_{min}, as shown in Fig. 1. The magnitude and phase angle limits constrain the tip of the voltage phasor to lie in the area bounded by the two semicircles having a radius of V_{min} and V_{max}, and the radial lines representing θ_{min} and θ_{max}. Phase angles have been assumed to lie in a very small range bounded by θ_{min} and θ_{max}. This assumption allows us to approximate the area available to the tip of voltage phasor by a pentagon $abcde$ having sides $L_1 - L_5$ [33]. There are two more reasons behind limiting the phase angles. Firstly, a large difference in the phase angle of different buses will lead to larger power flow which, in turn, may trigger instability, which is undesirable. The second reason is to maintain the validity of the assumption inherent in the conventional droop control equations (1) and (2). An assumption of smaller angle differences between the bus voltages has been made while deriving (1) and (2) from the power flow equations [34].

Referring to Fig. 1, the equations defining the line segments $L_1 - L_5$ can be easily found after knowing the points of intersection of these lines with the two semicircles. The

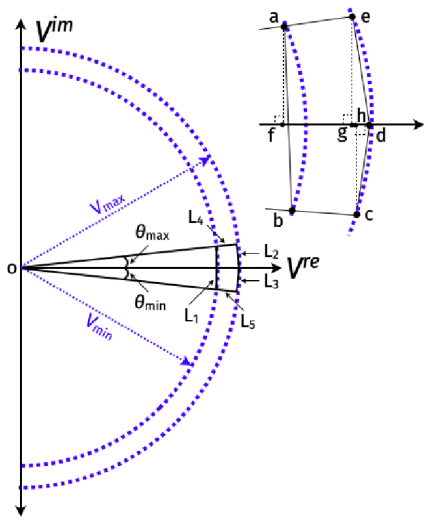


Fig. 1: Magnitude and angle limit for the bus voltage: approximation using line $L_1 - L_5$

resultant expressions for the line segments $L_1 - L_5$ are expressed as follows:

$$L_1 \Rightarrow V_i^{im} \leq \frac{\sin\ \theta_{max} - \sin\ \theta_{min}}{\cos\ \theta_{max} - \cos\ \theta_{min}}(V_i^{re} + V_{min}\cos\theta_{min}) + V_{min}\ \sin\ \theta_{min} \tag{18}$$

$$L_2 \Rightarrow V_i^{im} \leq \frac{\sin\ \theta_{max}}{\cos\ \theta_{max} - 1}(V_i^{re} - V_{max}) \tag{19}$$

$$L_3 \Rightarrow V_i^{im} \geq \frac{\sin\ \theta_{min}}{\cos\ \theta_{min} - 1}(V_i^{re} - V_{max}) \tag{20}$$

$$L_4 \Rightarrow V_i^{im} \leq V_i^{re}\ \tan\ \theta_{max} \tag{21}$$

$$L_5 \Rightarrow V_i^{im} \geq V_i^{re}\ \tan\ \theta_{min} \tag{22}$$

It can be seen from the zoomed portion of Fig. 1 that the length of the line segment "of" is now the effective lower bound for V^{re}. Hence, instead of V_{min}, the lower bound of V^{re} (denoted as V_{min}^{re}) is set to be equal to the length of "of". V_{min}^{re} is set as follows:

$$V_{min}^{re} = V_{min}\ \cos\ \beta \tag{23}$$

where β is the absolute maxima between θ_{max} and θ_{min}. Please note that the zoomed portion of the Fig. 1 has been drawn assuming $|\theta_{max}| > |\theta_{min}|$. It is to be noted that V_{min}^{re} is slightly lesser than the radius V_{min}.

Similarly, the upper and the lower bound of V_{im}, denoted as V_{max}^{im} (length "eg") and V_{min}^{im} (length "ch") respectively, is calculated as follows:

$$V_{max}^{im} = V_{max}\ \sin\ \theta_{max} \tag{24}$$

$$V_{min}^{im} = -V_{max}\ \sin\ \theta_{min} \tag{25}$$

1949-3053 (c) 2020 IEEE. Personal use is permitted, but republication/redistribution requires IEEE permission. See http://www.ieee.org/publications_standards/publications/rights/index.html for more information.
Authorized licensed use limited to: Imperial College London. Downloaded on August 29,2020 at 19:16:47 UTC from IEEE Xplore. Restrictions apply.

This article has been accepted for publication in a future issue of this journal, but has not been fully edited. Content may change prior to final publication. Citation information: DOI 10.1109/TSG.2020.3017952, IEEE Transactions on Smart Grid

3) Load Modelling: The voltage magnitude has a profound effect on power consumption and the reactive power flow. Hence, a static load model, namely the ZIP model has been used to consider the effect of the voltage magnitude on power consumption [35]. The variation in the active and reactive components of the load, namely P_{l-i} and Q_{l-i}, with the change in the voltage magnitude, is given as follows:

$$P_{l-i} = P_{0l-i}\left[P_p + I_p\frac{V_i}{V_0} + Z_p\left(\frac{V_i}{V_0}\right)^2\right] \tag{26}$$

$$Q_{l-i} = Q_{0l-i}\left[P_q + I_q\frac{V_i}{V_0} + Z_q\left(\frac{V_i}{V_0}\right)^2\right] \tag{27}$$

and

$$Z_p + I_p + P_p = 1 \tag{28}$$

$$Z_q + I_q + P_q = 1 \tag{29}$$

where P_{0-li} and Q_{0-li} are the nominal power of the load. V_0 is the magnitude of the nominal value of the phase voltage, whereas V_i is the actual voltage at the bus i. Z_p, I_p, P_p, Z_q, I_q and P_q are the ZIP coefficients of the load.

The load current I_l can be expressed as follows:

$$I^{re}_{l-i} = \frac{P_{l-i}V^{re}_i + Q_{l-i}V^{im}_i}{1.5\left[(V^{re}_i)^2 + (V^{im}_i)^2\right]} \tag{30}$$

$$I^{im}_{l-i} = \frac{P_{l-i}V^{im}_i - Q_{l-i}V^{re}_i}{1.5\left[(V^{re}_i)^2 + (V^{im}_i)^2\right]} \tag{31}$$

Equation (30) and (31) are nonlinear and are approximated to a linear combination of V^{re}_i and V^{im}_i as follows:

$$I^{re}_{l-i} = a_{l-i}V^{re}_i + b_{l-i}V^{im}_i + c_{l-i} \tag{32}$$

$$I^{im}_{l-i} = d_{l-i}V^{re}_i + e_{l-i}V^{im}_i + f_{l-i} \tag{33}$$

The coefficients $a_l - f_l$ can be calculated for each load by using techniques such as linear regression or by linearising (30)−(31) around an operating point. A good linear fit between the current and the voltage is possible because the variation in the voltage magnitude and angle is relatively small [33], [36].

4) Droop Modelling: The droop equations (1) and (2) are not applicable to the buses where no DG gets placed. Rearranging (1) and (2), and inserting the correction terms ΔP_i and ΔQ_i, respectively, we get:

$$P_{s.i} = \frac{\omega_n}{m_{p.s.i}} - \frac{\omega_s}{m_{p.s.i}} + \Delta P_i \tag{34}$$

$$Q_{s.i} = \frac{V_{n.s.i}}{n_{q.s.i}} - \frac{V^{re}_{s.i}}{n_{q.s.i}} + \Delta Q_i \tag{35}$$

Variables ΔP_i and ΔQ_i have been introduced because the DG placement is not known in advance. Now, ΔP_i and ΔQ_i should be assigned a zero value if a DG is placed at a bus i. Inequality presented below in (36) and (37) are used to implement this condition. Thus, when $\lambda_{s.i} = 1$, both ΔP_i and ΔQ_i become equal to zero. Otherwise, ΔP_i and ΔQ_i need to be allowed to take a value in a wide range for getting a feasible solution. This is implemented as follows:

$$0 \le \Delta P_i \le M_{DG}(1 - \lambda_{s.i}) \tag{36}$$

$$-M_{DG}(1 - \lambda_{s.i}) \le \Delta Q_i \le M_{DG}(1 - \lambda_{s.i}) \tag{37}$$

where M_{DG} is a constant defined as follows.

$$M_{DG} = max\left\{\mid P^{max}_s \mid, \mid Q^{min}_s \mid, \mid Q^{max}_s \mid\right\} \tag{38}$$

Further, the maximum number of DGs is limited as follows:

$$\sum \lambda_{s.i} \le N_{max} \tag{39}$$

where N_{max} is the maximum number of DGs that are planned to be placed in the network.

It is to be noted that m_p and n_q are variables because their value depends on the sizes of the DGs; which itself are not known beforehand, and will be calculated by the optimisation. Hence, the ratios $\frac{\omega_s}{m_{p.s.i}}$, $\frac{V_{n.s.i}}{n_{q.s.i}}$ and $\frac{V^{re}_{.s.i}}{n_{q.s.i}}$ appearing in (34) and (35) are nonlinear. It should be pointed out that once the DG allocation is completed, then the sizes and locations of the DGs will become known. In other words, m_p and n_q become known for different DGs, and after that, these values can be taken as constants to perform optimal day-ahead dispatch. The following process has been followed to approximate the nonlinear ratios of (34) and (35) into a linear form.

Discretization of terms containing $\frac{1}{m_p}$ and $\frac{1}{n_q}$: $\frac{1}{m_p}$ can be discretized as follows. Let $\frac{1}{m_p}$ be a multiple of a factor called as b_{mp} and is expressed as follows:

$$b_{mp} = \frac{1}{S_m m_{p-st}} \tag{40}$$

where m_{p-st} is the lower bound for m_p. Thus, $\frac{1}{m_{p.s.i}}$ can be expressed as follows:

$$\frac{1}{m_{p.s.i}} = b_{mp}\sum_{p=1}^{S_m}\gamma_{m.p} \tag{41}$$

where $\gamma_{m.p}$ is a binary variable and S_m is a constant which decides the width of b_{mp}. It should be noted that a smaller value of b_{mp} is desired for greater accuracy in the approximation. A sufficiently small value for b_{mp} can be chosen by selecting a high enough value of S_m while also considering computational complexity and burden.

Now, the first term on the right-hand side of (34) can be written as follows:

$$\frac{\omega_n}{m_{p.s.i}} = \omega_n b_{mp}\sum_{p=1}^{S_m}\gamma_{m.p} \tag{42}$$

Similarly, the second ratio in (34) can be written as follows:

$$\frac{\omega_s}{m_{p.s.i}} = \omega_s b_{mp} + \sum_{p=1}^{S_m} C_\omega \tag{43}$$

1949-3053 (c) 2020 IEEE. Personal use is permitted, but republication/redistribution requires IEEE permission. See http://www.ieee.org/publications_standards/publications/rights/index.html for more information.
Authorized licensed use limited to: Imperial College London. Downloaded on August 29,2020 at 19:16:47 UTC from IEEE Xplore. Restrictions apply.

This article has been accepted for publication in a future issue of this journal, but has not been fully edited. Content may change prior to final publication. Citation information: DOI 10.1109/TSG.2020.3017952, IEEE Transactions on Smart Grid

where C_ω is defined as a product of ω_s and b_{mp} when $\gamma_{m.p} = 1$ else it is set to zero. This is implemented as follows:

$$0 \leq \omega_s b_{mp} - C_\omega \leq \omega_{max} b_{mp}(1 - \gamma_{m.p}) \tag{44}$$

$$0 \leq C_\omega \leq \omega_{max} b_{mp} \gamma_{m.p} \tag{45}$$

where ω_{max} is the maximum allowable frequency in the microgrid.

The output of the optimisation routine would provide us with the values related to the active and reactive power generation of all the DGs. However, these values should be rounded off to the nearest rating for each DG, e.g. in multiples of 100 kW. This can be implemented using the following expressions and as shown in Fig. 2.

$$P_\omega \sum_{p=1}^{S_m} \gamma_{m.p} \leq P_{s.i} \leq P_\omega \left(1 + \sum_{p=1}^{S_m} \gamma_{m.p}\right) \tag{46}$$

where P_ω is the lowest rating. The following condition needs to be enforced on $\gamma_{m.p}$.

$$\gamma_{m.p} \leq \gamma_{m.p(p-1)} \tag{47}$$

It can be observed from Fig. 2 that $\gamma_{m.p} = 1$ if and only if $\gamma_{m.p(p-1)} = 1$.

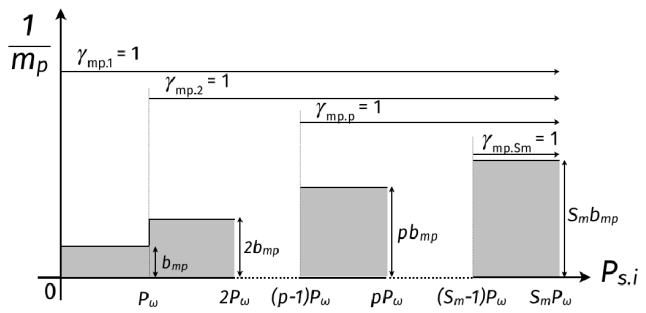


Fig. 2: Correlation of $\frac{1}{m_p}$ with P_s

A similar process has been followed to discretize terms containing $\frac{1}{n_q}$ and to obtain the reactive power rating of the DGs.

5) DG power calculation: The active and reactive power output of the DG is calculated as follows:

$$P_{s.i} = 1.5\ (V_i^{re} I_{s.i}^{re} + V_i^{im} I_{s.i}^{im}) \tag{48}$$

$$Q_{s.i} = 1.5\ (V_i^{im} I_{s.i}^{re} - V_i^{re} I_{s.i}^{im}) \tag{49}$$

The power limits for the DGs are defined as follows:

$$0 \leq P_{s.i} \leq P_s^{max} \tag{50}$$

$$Q_s^{min} \leq Q_{s.i} \leq Q_s^{max} \tag{51}$$

The power factor of each DG also needs to be bounded as follows [37]:

$$pf_{s.i} \geq pf_{min} \tag{52}$$

Equations (48) and (49) are nonlinear because of the presence of product terms of voltage and current. Thus, these four product terms should be linearised. The description of the process followed for linearising these product terms has been shifted to the appendix section for maintaining the flow of discussion. Lastly, the output current of each DG is limited as follows:

$$0 \leq I_{s.i}^{re} \leq I_{max}^{re} \lambda_{s.i} \tag{53}$$

$$-I_{max}^{im} \lambda_{s.i} \leq I_{s.i}^{im} \leq I_{max}^{im} \lambda_{s.i} \tag{54}$$

6) Incorporating reconfiguration: The KVL equations presented in (14)−(15) should be modified as follows to consider reconfiguration:

$$V_i^{re} = V_j^{re} + R_{ij} I_{ij}^{re} - X_{ij} I_{ij}^{im} + \Delta V_{ij}^{re} \tag{55}$$

$$V_i^{im} = V_j^{im} + X_{ij} I_{ij}^{re} + R_{ij} I_{ij}^{im} + \Delta V_{ij}^{im} \tag{56}$$

The ΔV_{ij}^{re} and ΔV_{ij}^{im} terms should be set to zero when the reconfiguration switch or the tie line switch is closed. On the other hand, ΔV_{ij} should be set equal to $V_i - V_j$ when the switch is open. This logic can be realised as follows:

$$-\Delta V_{max}^{re}(1 - Y_{ij}) \leq \Delta V_{ij}^{re} \leq \Delta V_{max}^{re}(1 - Y_{ij}) \tag{57}$$

$$-\Delta V_{max}^{im}(1 - Y_{ij}) \leq \Delta V_{ij}^{im} \leq \Delta V_{max}^{im}(1 - Y_{ij}) \tag{58}$$

where Y_{ij} is a binary variable denoting the status of the reconfiguration switches and the tie line switches present in the branch *ij*. $Y_{ij} = 1$ denotes that the switch is closed and $Y_{ij} = 0$ denotes that the switch is open.

From (57) and (58), when $Y_{ij} = 1$, ΔV_{ij}^{re} and ΔV_{ij}^{im} becomes zero. On the other hand, when $Y_{ij} = 0$, ΔV_{ij}^{re} and ΔV_{ij}^{im} is allowed to take a value from a wide range defined using $\pm\Delta V_{max}^{re}$ and $\pm\Delta V_{max}^{im}$ respectively. Here ΔV_{max} refers to the maximum possible voltage difference which can occur between a pair of a bus with no direct connection between them. Referring to Fig. 1 and equation (23), ΔV_{max}^{re} can be computed as follows:

$$\Delta V_{max}^{re} = V_{max} - V_{min}^{re} \tag{59}$$

Similarly, referring to Fig. 1 and equation (24), ΔV_{max}^{im} can be set to double of V_{max}^{im} as follows:

$$\Delta V_{max}^{im} = 2\ V_{max}\ \sin\ \beta \tag{60}$$

Now, the direction of branch currents may reverse due to application of reconfiguration. Hence, the limits imposed on the branch currents in (10)−(11) also need to be modified as follows:

$$-I_{max}^{re} Y_{ij} \leq I_{ij}^{re} \leq I_{max}^{re} Y_{ij} \tag{61}$$

$$-I_{max}^{im} Y_{ij} \leq I_{ij}^{im} \leq I_{max}^{im} Y_{ij} \tag{62}$$

The above constraints also ensure that the current limit for any open branch (reconfiguration branch or tie line) is strictly set to zero.

1949-3053 (c) 2020 IEEE. Personal use is permitted, but republication/redistribution requires IEEE permission. See http://www.ieee.org/publications_standards/publications/rights/index.html for more information.
Authorized licensed use limited to: Imperial College London. Downloaded on August 29,2020 at 19:16:47 UTC from IEEE Xplore. Restrictions apply.

This article has been accepted for publication in a future issue of this journal, but has not been fully edited. Content may change prior to final publication. Citation information: DOI 10.1109/TSG.2020.3017952, IEEE Transactions on Smart Grid

There are few critical concerns for successfully operating a microgrid, namely protective relay coordination and maintaining stability. These aspects are challenging, especially in a reconfigurable microgrid structure. It is well known that maintaining a radial structure instead of allowing mesh formation can greatly simplify the relay coordination [38]; in addition, it can also help in improving the stability margin [39]. Thus, the following constraint has been added to ensure radial structure in the microgrid [30], [33], [40]:

$$\sum_{1}^{N_{br}} Y_{ij} = N_b - 1 \tag{63}$$

where N_{br} is the total number of branches (including the reconfiguration branches) in the given network.

7) Modelling power loss limit: The real power losses (P_{loss}) in the branches needs to be kept to the minimal. It is well known that the line losses are affected by the voltage profile of the network, which in turn depends on the reactive power flow. Hence, it becomes essential to observe the line loss and the voltage profile while optimising for reactive power sharing. However, the optimisation formulation would become complex if line loss minimisation is also considered as an additional objective along with reactive power sharing objective. This stems from the fact that multi-objective optimisation is more complicated in general with regards to the formulation (e.g. assigning weights, mixing of units) as compared to a single objective optimisation. To avoid such complexities and also to keep the focus of the paper on the reactive power sharing concept, P_{loss} has been taken as a constraint with a very low value. Hence, any solution satisfying this constraint would give a "near-optimal" solution with regard to power losses also.

P_{loss} can be defined as follows:

$$P_{loss} = \sum_{0}^{N_{br}} 3\,(I_{ij}^{rms})^2 R_{ij} \tag{64}$$

P_{loss} is bounded as follows:

$$P_{loss} \leq P_{loss-max} \tag{65}$$

Generally, the optimal P_{loss} is of the order of $4-8\%$ of the nominal load for active distribution networks [24], [41] and is $0.5-1.5\%$ for island microgrids [42]. Thus, setting a lower bound of 1% for P_{loss} during optimisation would be reasonable.

Now, $(I_{ij}^{rms})^2$ being a square term is nonlinear and needs to be approximated with an equivalent linear expression. The steps followed to linearise $(I_{ij}^{rms})^2$ are as follows [43]:

$$(I_{ij}^{rms})^2 = \left(\frac{|I_{ij}|}{\sqrt{2}}\right)^2 = \frac{(I_{ij}^{re})^2 + (I_{ij}^{im})^2}{2} \tag{66}$$

because

$$I_{ij} = I_{ij}^{re} + jI_{ij}^{im} \tag{67}$$

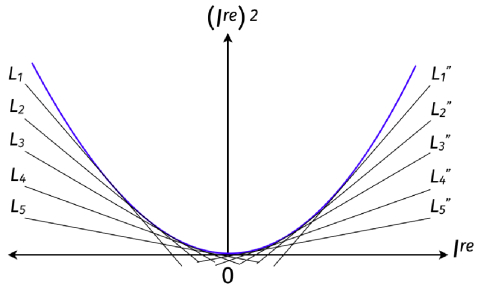


Fig. 3: Approximating $(I_{ij}^{re})^2$ with tangents

$(I_{ij}^{re})^2$ (or $(I_{ij}^{im})^2$) can be represented as a parabola, as shown in Fig. 3. This parabola can be approximated by a piecewise linearisation using N_{li} number of tangents as follows:

$$(I_{ij}^{re})^2 \geq a_{re} I_{ij}^{re} + b_{re} \tag{68}$$

where the a_{re} and b_{re} are the slopes and intercepts of the tangents. Similarly, $(I_{ij}^{im})^2$ is approximated as follows:

$$(I_{ij}^{im})^2 \geq a_{im} I_{ij}^{im} + b_{im} \tag{69}$$

Ten lines have been shown in Fig. 3. A sufficiently higher number of lines should be used to increase the accuracy of the approximation.

III. Results and Discussion

The proposed MILP formulation for optimal allocation and dispatch has been validated on a modified 33 bus distribution network [44]. The original system has a grid connection at bus 1. The grid connection has been removed to form an islanded microgrid, as shown in Fig. 4. The 33 bus system is widely used in the literature for validating optimisation formulations [37], [45], especially for those involving reconfiguration [26], [30]. The network and the load parameters are kept the same as in [44]. The nominal voltage level of the network is 12.66 kV, 50 Hz and the total nominal load is 3.7 MW and 2.3 Mvar. It is to be noted that only one load level corresponding to the peak value has been considered for the DG sizing and placement part. However, multiple load levels can be incorporated conveniently. The network contains five reconfiguration switches (in branch $33-37$) as shown in Fig. 4.

Table I: ZIP coefficients for residential and industrial loads

Load Type	Z_p	I_p	P_p	Z_q	I_q	P_q
Residential	1.31	-1.94	1.63	9.20	-15.27	7.07
Industrial	1.21	-1.61	1.40	4.36	-7.08	3.72

The loads have been modelled as residential loads (bus $1-22$) and industrial loads (bus $23-33$) as marked in Fig. 4. This has been implemented by considering appropriate values of ZIP coefficients for these types of loads [46].

1949-3053 (c) 2020 IEEE. Personal use is permitted, but republication/redistribution requires IEEE permission. See http://www.ieee.org/publications_standards/publications/rights/index.html for more information.
Authorized licensed use limited to: Imperial College London. Downloaded on August 29,2020 at 19:16:47 UTC from IEEE Xplore. Restrictions apply.

This article has been accepted for publication in a future issue of this journal, but has not been fully edited. Content may change prior to final publication. Citation information: DOI 10.1109/TSG.2020.3017952, IEEE Transactions on Smart Grid

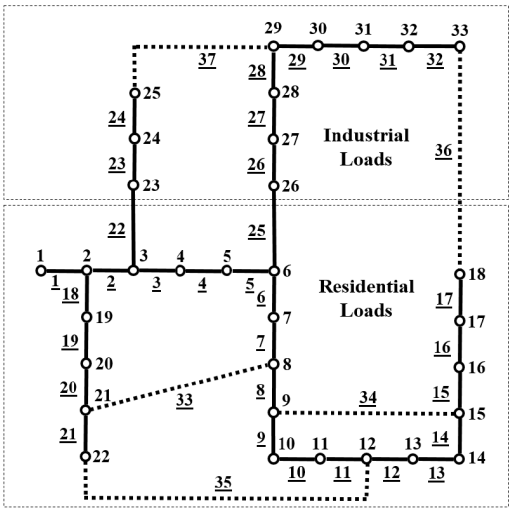


Fig. 4: Modified 33 bus microgrid

Table II: Parameters used for case studies

Parameter	Value	Unit
ω_n	314.16	rad/s
ω_{min}	0.99	p.u.
P_s^{max}	1	MW
Q_s^{min}, Q_s^{max}	-1, 1	Mvar
pf_{min}	0.7	–
θ_{min}, θ_{max}	$-5°$, 4°	–
V_{min}, V_{max}	0.95, 1.05	p.u.
I_{max}	400	A
N_{max}	10	–
K	15	–
S_m	10	–
N_{li}	40	–
$P_{loss-max}$	37.15	kW
m_{p-st}	1e$-$7	rad/s/W
n_{q-st}	1e$-$5	V/var

These values are reproduced in Table I for reference. The total consumption of the residential section is 1.86 MW, 0.9 Mvar, whereas the consumption of industrial section is 1.85 MW and 1.4 Mvar. The loads have been considered as either constant impedance load or as ZIP loads to show the difference in reactive power sharing due to load modelling. Linear fitting of I_l^{re} and I_l^{im} has been performed in terms of V_i^{re} and V_i^{im} respectively. The coefficients $a_l - f_l$ have been obtained for each load by using the *regress* function of MATLAB. The data used for the fitting has been generated by considering a range of $0.9-1$ pu for the voltage magnitude, and a range of $-6°$ to $5°$ for the phase angle, respectively. The R^2 values obtained for the fitting were close to 1. It is to be noted that the approximation discussed in $(32)-(33)$ can introduce a non-negligible error if the voltage value lies significantly outside the range which has been considering for fitting.

All the relevant parameters used for the case studies are as listed in Table II. A deviation of $\pm 5\%$ from the nominal has been considered for $V_{n.s.i}$. The MILP model has been implemented in MATLAB and has been solved using CPLEX solver.

A. Effect of considering loss minimisation as an objective

In this case, the reactive power sharing performance has been assessed if the optimal allocation of DGs is obtained by considering the line loss minimisation as an objective (as expressed in (64)). This case has been executed considering ZIP loads and without considering the reconfiguration option. A line loss of 1.19 kW is obtained. The power outputs and the reactive power sharing errors are as shown in Table III. The expected proportional reactive power output of each DG (Q_{s-exp}) is calculated as follows:

$$Q_{s-exp} = \frac{\sum Q_s}{\sum P_s} \times P_s \tag{70}$$

The reactive power sharing error (Q_{s-err}) for each DG can be expressed as follows:

$$\%Q_{s-err} = \frac{Q_s - Q_{s-exp}}{Q_{s-exp}} \times 100 \tag{71}$$

A near-zero value of $\%Q_{s-err}$ for all the DGs indicates a perfect reactive power sharing. It is observed from Table III that the $\%Q_{s-err}$ is far from zero. In particular, Q_s of DGs located at bus 30 and 32 exceed their respective Q_{s-exp} by 75% and 65% respectively. Thus, these DGs would get overloaded and may trip. This may lead to cascaded tripping of the remaining DGs. Hence, it is vital to consider proportional power sharing amongst DGs along with line losses while performing optimal DG allocation.

Table III: Power sharing amongst DGs considering the loss minimisation objective only

DG Bus	3	7	10	14	17	21	24	25	30	32
P_s (kW)	429	552	245	245	184	306	429	429	490	306
Q_s (kvar)	201	266	105	111	75	143	251	161	500	294
Q_{s-exp} (kvar)	250	322	143	143	107	179	250	250	286	179
Q_{s-err} (%)	-20	-17	-26	-22	-30	-20	0	-36	75	65

B. Optimal allocation of DGs and the effect of load modelling

In this subsection, the impact of considering a proper load model (ZIP) on the optimal allocation results versus considering a simplistic constant Z load model is discussed. Here onwards, proportional reactive power sharing has been considered as the objective function in all the case studies. The P_{loss} value is constrained to less than 1% of the total nominal active power load of the microgrid, as discussed in (65). The results obtained are as provided in Table IV. It can be observed from the values of Q_{s-err} in Table IV that the proposed formulation is able to achieve almost perfect proportional reactive power sharing for all the test cases. The maximum Q_{s-err} observed is -1.1%.

1949-3053 (c) 2020 IEEE. Personal use is permitted, but republication/redistribution requires IEEE permission. See http://www.ieee.org/publications_standards/publications/rights/index.html for more information.
Authorized licensed use limited to: Imperial College London. Downloaded on August 29,2020 at 19:16:47 UTC from IEEE Xplore. Restrictions apply.

This article has been accepted for publication in a future issue of this journal, but has not been fully edited. Content may change prior to final publication. Citation information: DOI 10.1109/TSG.2020.3017952, IEEE Transactions on Smart Grid

The key parameters summarising our observations are listed in Table V. Using a constant impedance load model instead of a ZIP model (case (a) versus (b)) would cause the following issues. Firstly, it would cause suboptimal reactive power sharing. Secondly, this would lead to the installation of more number of DGs than required (ten versus nine). In addition, the combined installed capacity of the DGs would be lower than the actual requirement (4.6 MVA instead of 4.7 MVA). Also, the actual line loss would be more than expected (17.2 kW instead of 10.6 kW). Thus, it is essential to use a ZIP model instead of a constant impedance model for loads to obtain a realistic solution.

C. Improved results by incorporating reconfiguration

Reconfiguration is widely applied for improving network performance in terms of reduced line losses, improved voltage profile and reduced loading of lines. The results for the case (c) (ZIP load model and reconfiguration) are as shown in Table IV and V. It can be seen that incorporating reconfiguration brings in additional benefits in terms of reduced line losses and improved voltage profile while simultaneously achieving proportional reactive power sharing. Besides, the number of DG units are also reduced further (from nine to seven).

D. Importance of considering the loss constraint

To understand the effect of loss constraint, the DG allocation study of case (a) has been repeated with no upper bound on P_{loss}. The results (case (d)) are as shown in Table IV and V. It can be observed from Table V that with no loss constraint in place, the line loss performance worsens as compared to the case (a). A deteriorated behaviour is also observed in the voltage range. Thus, it is important to consider the line loss constraint while optimising for reactive power sharing. It is also worth noting that a very low power loss ($0.29-1.26\%$, as seen for case (a)-(c)) can be achieved even without considering it as an optimisation objective.

E. Assessing the effectiveness and accuracy of the proposed optimisation formulation

The correctness and the accuracy of the proposed formulation have been verified by simulating the modified 33 bus microgrid with the results obtained from DG allocation cases. The simulation model has been built and executed in MATLAB/Simulink by using the blocks from its *SimPowerSystems* toolbox. It is to be noted that the line and load data used for simulation are exactly the same as used for optimisation.

It is observed that the current, voltage and the power values obtained from the optimisation routine almost matched with the values obtained from the corresponding simulation. To save space, only the P−Q outputs of the DGs for the case (c) have been included, as shown in Fig. 5 and Table VI. It is observed that the difference between the P−Q outputs obtained from the optimisation and simulation is negligible (a maximum difference of 1.39% is observed). Also, the difference in the power loss value obtained from the optimisation (10.7 kW) and simulation (10.6 kW) is also negligible. This confirms the correctness of the proposed formulation and validates the accuracy of the various linearisation which have been applied.

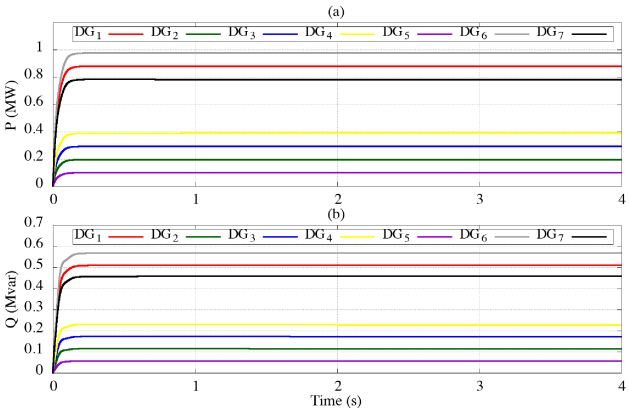


Fig. 5: Simulation result: PQ outputs of all DGs for case (c)

A negligible difference between the optimisation and the simulation values has been possible because of a judicious setting of the following variables: N_{li}, S_m and K. To show the effect of the choice of values of N_{li}, S_m and K on the accuracy of the results, a case study has been performed with a setting of 20% lesser values for these variables as compared to their values listed in Table II. Hence, $N_{li} = 32$, $S_m = 8$ and $K = 12$ has been set to repeat the DG allocation of case (c). The difference between the P−Q outputs obtained from the optimisation and the simulation is as shown in Table VII. It can be seen that the difference in the P−Q values are appreciably high (as high as -21.57%), and hence the accuracy of the approximations is unacceptable with the chosen values of N_{li}, S_m and K. A higher value for these parameters would improve the accuracy. However, it would also lead to an increase in the computational burden.

F. Applying unequal capacity constraint for different buses

An equal constraint on capacity (1 MVA and ± 1 Mvar) has been considered for DG allocation cases (a)−(d) for the sake of understanding. As seen from the results of these cases, it is observed that there is a trade-off between the number of DGs being placed and their sizes. It can be seen that a lesser number of DGs correspond to bigger DGs getting placed and vice versa. However, in practice, there may be a need to restrict the size of the DGs either for each bus or for a group of buses.

In case (e), the DG allocation is performed by considering different capacity constraints for buses located in different

1949-3053 (c) 2020 IEEE. Personal use is permitted, but republication/redistribution requires IEEE permission. See http://www.ieee.org/publications_standards/publications/rights/index.html for more information.
Authorized licensed use limited to: Imperial College London. Downloaded on August 29,2020 at 19:16:47 UTC from IEEE Xplore. Restrictions apply.

This article has been accepted for publication in a future issue of this journal, but has not been fully edited. Content may change prior to final publication. Citation information: DOI 10.1109/TSG.2020.3017952, IEEE Transactions on Smart Grid

Table IV: Output of optimal allocation of DGs: locations and sizes

(a) Z without reconfiguration	DG Bus	3	7	9	13	16	18	23	24	31	32
	DG size (kVA)	1000	200	500	200	200	300	500	600	800	300
	P_s (kW)	851	95	378	95	95	189	378	473	662	189
	Q_s (kvar)	522	58	232	58	58	116	232	290	406	116
	Q_{s-err} (%)	0.03	−0.44	0.09	−0.44	−0.44	0.09	0.09	−0.02	0.01	0.09
	m_p (rad/s/W)	1.11e−7	1.00e−6	2.50e−7	1.00e−6	1.00e−6	5.00e−7	2.50e−7	2.00e−7	1.43e−7	5.00e−7
	n_q (V/var)	1.11e−5	1.00e−4	2.50e−5	1.00e−4	1.00e−4	5.00e−5	2.50e−5	2.00e−5	1.43e−5	5.00e−5
(b) ZIP without reconfiguration	DG Bus	4	8	10	18	19	24	25	29	32	–
	DG size (kVA)	200	300	600	300	200	800	1100	800	400	–
	P_s (kW)	98	197	492	197	98	689	886	689	295	–
	Q_s (kvar)	57	114	286	114	57	401	515	401	172	–
	Q_{s-err} (%)	0.03	−0.47	−0.02	−0.47	0.03	0.10	−0.03	0.10	0.28	–
	m_p (rad/s/W)	1.00e−6	5.00e−7	2.00e−7	5.00e−7	1.00e−6	1.43e−7	1.11e−7	1.43e−7	3.33e−7	–
	n_q (V/var)	1.00e−4	5.00e−5	2.00e−5	5.00e−5	1.00e−4	1.43e−5	1.11e−5	1.43e−5	3.33e−5	–
(c) ZIP with reconfiguration	DG Bus	3	11	13	20	23	25	32	–	–	–
	DG size (kVA)	1100	300	400	500	200	1200	1000	–	–	–
	P_s (kW)	879	195	293	391	98	977	782	–	–	–
	Q_s (kvar)	517	115	172	230	57	575	460	–	–	–
	Q_{s-err} (%)	0.01	0.28	−0.18	0.02	−1.10	0.07	0.02	–	–	–
	m_p (rad/s/W)	1.11e−7	5.00e−7	3.33e−7	2.50e−7	1.00e−6	1.00e−7	1.25e−7	–	–	–
	n_q (V/var)	1.11e−5	5.00e−5	3.33e−5	2.50e−5	1.00e−4	1.00e−5	1.25e−5	–	–	–
	Open branches	8, 9, 18, 21, 23									
(d) Z without reconfiguration, (no loss constraint)	DG Bus	2	6	18	24	27	32	33	–	–	–
	DG size (kVA)	400	1000	300	600	100	1000	900	–	–	–
	P_s (kW)	305	839	229	458	76	839	763	–	–	–
	Q_s (kvar)	190	523	143	285	47	523	475	–	–	–
	Q_{s-err} (%)	0.00	0.06	0.24	−0.11	−0.73	0.06	−0.07	–	–	–
	m_p (rad/s/W)	2.50e−7	9.09e−8	3.33e−7	1.67e−7	1.00e−6	9.09e−8	1.00e−7	–	–	–
	n_q (V/var)	2.50e−5	9.09e−6	3.33e−5	1.67e−5	1.00e−4	9.09e−6	1.00e−5	–	–	–
(e) Z without reconfiguration (section-wise capacity constraint)	DG Bus	4	7	12	13	18	19	22	23	30	33
	DG size (kVA)	500	500	400	100	500	600	300	1000	900	400
	P_s (kW)	424	424	283	71	354	495	212	778	707	283
	Q_s (kvar)	264	264	176	44	220	308	132	484	440	176
	Q_{s-err} (%)	0.09	0.09	0.10	0.09	0.09	0.10	0.10	0.10	0.09	0.10
	m_p (rad/s/W)	1.67e−7	1.67e−7	2.50e−7	1.00e−6	2.00e−7	1.43e−7	3.33e−7	9.09e−8	1.00e−7	2.50e−7
	n_q (V/var)	1.67e−5	1.67e−5	2.50e−5	1.00e−4	2.00e−5	1.43e−5	3.33e−5	9.09e−6	1.00e−5	2.50e−5

Table V: Comparison of all cases on key parameters

Case	No. of DGs	$\sum P_s$ (MW)	$\sum Q_s$ (Mvar)	$\sum S_s$ (MVA)	$\sum$ DG Rating (MVA)	P_{loss} (kW)	I_{ij-max} (A)	V_{i-min} (p.u.)	V_{i-max} (p.u.)
(a) Z without reconfiguration	10	3.41	2.09	4.00	4.6	10.6 (0.29%)	27	0.951	0.958
(b) ZIP without reconfiguration	9	3.64	2.12	4.21	4.7	17.2 (0.46%)	43	0.952	0.972
(c) ZIP with reconfiguration	7	3.62	2.13	4.20	4.7	10.7 (0.29%)	39	0.950	0.964
(d) Z without reconfiguration (no loss constraint)	7	3.51	2.18	4.13	4.3	46.8 (1.26%)	72	0.952	1.003
(e) Z without reconfiguration (section-wise capacity constraint)	10	4.03	2.51	4.75	5.2	12.4 (0.33%)	44	1.034	1.049

Table VI: Difference between optimisation results and simulation for case (c) for $N_{li} = 40$, $S_m = 10$ and $K = 15$

	Optimisation		Simulation		Difference	
DG no.	P_s (kW)	Q_s (kvar)	P_s (kW)	Q_s (kvar)	P_s (%)	Q_s (%)
DG_1	879.5	517.1	878.0	510.0	0.17	1.37
DG_2	195.4	114.9	194.9	113.9	0.26	0.87
DG_3	293.2	172.4	292.4	171.8	0.27	0.35
DG_4	390.9	229.8	390.0	227.2	0.23	1.13
DG_5	97.7	57.5	97.6	56.7	0.10	**1.39**
DG_6	977.2	574.6	975.6	567.5	0.16	1.24
DG_7	781.8	459.8	780.2	458.0	0.20	0.39

Table VII: Difference between optimisation results and simulation for case (c) for $N_{li} = 32$, $S_m = 8$ and $K = 12$

	Optimisation		Simulation		Difference	
DG no.	P_s (kW)	Q_s (kvar)	P_s (kW)	Q_s (kvar)	P_s (%)	Q_s (%)
DG_1	125.0	72.8	124.4	74.3	0.43	−2.00
DG_2	125.0	72.8	124.4	73.2	0.43	−0.65
DG_3	249.9	145.5	248.9	145.1	0.40	0.34
DG_4	374.9	218.3	373.3	217.1	0.41	0.54
DG_5	499.8	291.1	497.8	288.3	0.40	0.95
DG_6	874.7	509.4	871.3	509.9	0.39	−0.10
DG_7	374.9	218.3	373.1	236.8	0.48	−7.80
DG_8	749.7	436.6	745.6	375.8	0.56	16.19
DG_9	249.9	145.5	248.4	185.6	0.60	**−21.57**

sections (residential and industrial). A DG capacity limit of 500 kVA and ±500 kvar has been considered for the residential section (bus 1−22), and a limit of 1 MVA and

1949-3053 (c) 2020 IEEE. Personal use is permitted, but republication/redistribution requires IEEE permission. See http://www.ieee.org/publications_standards/publications/rights/index.html for more information.
Authorized licensed use limited to: Imperial College London. Downloaded on August 29,2020 at 19:16:47 UTC from IEEE Xplore. Restrictions apply.

This article has been accepted for publication in a future issue of this journal, but has not been fully edited. Content may change prior to final publication. Citation information: DOI 10.1109/TSG.2020.3017952, IEEE Transactions on Smart Grid

± 1 Mvar has been considered for the industrial section (bus 23−33) of the microgrid respectively. It is observed that the number of DGs getting placed remain the same as the case (a) whereas the DG sizes have increased. Moreover, the total power consumption is more as compared to the case (a) due to higher voltage magnitude.

G. Using optimal allocation results for optimal day−ahead dispatch

The results of the optimal allocation of the DGs can be utilised to perform a day-ahead optimal volt-var dispatch for DGs and to schedule the reconfiguration switches. Values of the following variables are known at the end of the optimal sizing-siting study, namely, m_p and n_q (relates to the size of DGs), and λ_s (location of DGs). Hence, these variables are treated as constants while formulating for the day-ahead dispatch. Besides, correction terms such as V_ϵ^q, ΔP_i and ΔQ_i are no longer needed. Moreover, the process followed to linearise the nonlinear ratios $\frac{\omega_s}{m_{p.s.i}}$, $\frac{V_{n.s.i}}{n_{q.s.i}}$ and $\frac{V^{re}_{.s.i}}{n_{q.s.i}}$ appearing in (34) and (35), and its related equations/variables are also no longer needed for formulating the day-ahead optimal dispatch. Thus, in effect, except for the changes mentioned above, the same set of equations as used for the allocation is used for the day-ahead dispatch.

An hourly forecast of residential and industrial loads, as shown in Fig. 6 has been used. The optimal dispatch and scheduling are executed in a central controller. The central controller communicates the V_n setpoint to each DG, and it also schedules the status of the tie switches/reconfiguration switches. The V_n setpoints and the branch status obtained using results of the case (c) are as shown in Table VIII. The resultant voltage profile across the microgrid is as shown in Fig. 7. An almost perfect reactive power sharing amongst DGs has been achieved for all the hours as seen from the $\%Q_{s-err}$ values in Table IX. The maximum Q_{s-err} observed is 2.04%. The observed line losses over the whole day is 201 kWh.

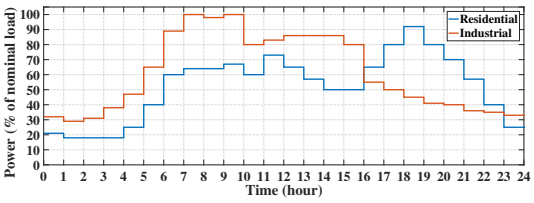


Fig. 6: 24 hour load profile: residential and industrial loads

H. Comparing the performance of the proposed formulation

To understand the significance and value of considering reactive power sharing during the planning stage itself, it is important to first understand as to why an arbitrary allocation of DG worsens the performance. A 38 bus microgrid has been used for this purpose. The rated voltage of the network is 380 V, 50 Hz and the total nominal load is 120 kW and 63 kvar. The line and the load parameters have been referred from [19]. It can be observed from Table X that, for an arbitrary sizing and placement of DGs, the average Q_{s-err} for the DGs is 63.6% which is far from acceptable. It can be further seen that the average Q_{s-err} almost halves to 31.2% just by optimising the location and size of the DGs. Thus, an optimal DG allocation can alleviate the problem of reactive power sharing to a great extent. Further, the reactive power sharing becomes near perfect when the DG allocation is followed by an optimal volt-var dispatch. In addition, DG allocation followed by volt-var dispatch also improves the line loss and voltage performance.

Table VIII: Day−ahead dispatch: V_n setpoints and reconfiguration switch/tie switch schedule

	V_n							Open Branches
Hour	DG_1	DG_2	DG_3	DG_4	DG_5	DG_6	DG_7	
1	1.041	1.043	1.044	1.043	1.041	1.040	1.040	8, 14, 16, 18, 27
2	1.039	1.041	1.041	1.039	1.039	1.037	1.043	4, 9, 19, 21, 30
3	1.041	1.043	1.044	1.042	1.041	1.041	1.041	6, 9, 14, 16, 24
4	1.048	1.046	1.047	1.047	1.047	1.045	1.045	4, 11, 15, 21, 28
5	0.954	0.951	0.951	0.951	0.953	0.952	0.953	3, 10, 27, 32, 34
6	1.044	1.041	1.041	1.043	1.043	1.040	1.040	5, 11, 19, 25, 35
7	1.040	1.044	1.044	1.043	1.039	1.038	1.038	7, 9, 12, 16, 28
8	1.034	0.995	0.997	1.022	1.034	0.953	1.008	3, 12, 23, 31, 33
9	1.048	1.045	1.045	1.048	1.046	1.040	1.039	4, 6, 11, 16, 21
10	1.047	1.041	1.045	1.047	1.044	1.038	1.046	3, 13, 26, 30, 33
11	1.042	1.044	1.044	1.043	1.041	1.040	1.041	7, 9, 12, 16, 28
12	1.046	1.036	1.036	1.041	1.046	1.046	1.048	5, 11, 25, 34, 36
13	0.953	0.953	0.952	0.955	0.952	0.950	0.950	2, 7, 9, 27, 33
14	1.045	1.036	1.035	1.043	1.045	1.049	1.039	6, 9, 21, 32, 37
15	1.034	1.046	1.047	1.040	1.031	1.022	1.023	5, 9, 14, 30, 33
16	1.041	1.043	1.042	1.044	1.040	1.044	1.046	9, 19, 24, 32, 35
17	1.043	1.044	1.045	1.044	1.042	1.046	1.045	2, 8, 14, 24, 33
18	1.040	1.036	1.037	1.036	1.041	1.046	1.024	7, 10, 14, 29, 37
19	1.048	1.035	1.035	1.043	1.048	1.044	1.045	5, 12, 16, 23, 35
20	1.044	1.030	1.028	1.038	1.044	1.041	1.045	4, 11, 12, 23, 36
21	1.044	1.046	1.046	1.045	1.045	1.047	1.048	8, 9, 26, 33, 35
22	1.048	1.044	1.044	1.046	1.047	1.046	1.046	5, 7, 11, 34, 35
23	1.042	1.037	1.038	1.041	1.042	1.040	1.039	4, 14, 21, 24, 34
24	1.046	1.044	1.044	1.048	1.045	1.046	1.046	16, 20, 21, 24, 34

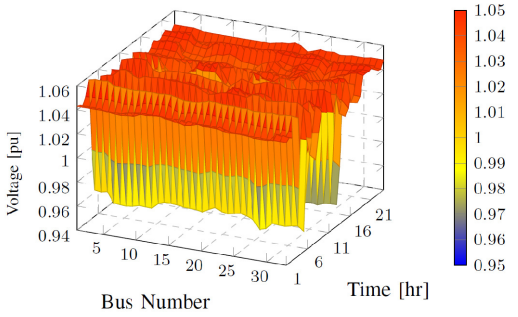


Fig. 7: Voltage profile for the whole day

IV. Conclusion

A MILP formulation has been proposed to obtain optimal DG allocation and dispatch schedule for achieving proportional reactive power sharing amongst DGs, while incurring very low line losses. In addition, the effect of different load models has been studied. Furthermore, network reconfig-

1949-3053 (c) 2020 IEEE. Personal use is permitted, but republication/redistribution requires IEEE permission. See http://www.ieee.org/publications_standards/publications/rights/index.html for more information.
Authorized licensed use limited to: Imperial College London. Downloaded on August 29,2020 at 19:16:47 UTC from IEEE Xplore. Restrictions apply.

This article has been accepted for publication in a future issue of this journal, but has not been fully edited. Content may change prior to final publication. Citation information: DOI 10.1109/TSG.2020.3017952, IEEE Transactions on Smart Grid

Table IX: Day−ahead dispatch: $Q_{s-err}\%$ of all the DGs over the whole day

Hour	DG_1	DG_2	DG_3	DG_4	DG_5	DG_6	DG_7
1	0.19	0.84	0.75	−0.56	0.56	0.22	0.07
2	0.00	0.63	0.63	0.79	0.63	0.06	−0.08
3	−0.27	−1.20	−0.20	0.30	1.80	0.00	0.30
4	0.00	1.01	−0.51	−0.13	1.01	0.10	−0.13
5	−0.05	0.00	0.00	0.00	0.00	0.00	0.00
6	−0.03	−0.14	0.28	−0.21	1.12	0.11	0.18
7	0.02	−0.40	0.27	0.10	−0.40	−0.02	0.07
8	−0.08	0.38	−0.32	−0.14	0.38	−0.04	0.12
9	−0.06	0.27	−0.06	−0.18	−0.72	0.07	0.02
10	0.10	−0.18	0.12	−0.18	0.71	−0.02	0.02
11	0.07	−0.53	−0.14	0.00	0.64	−0.09	0.03
12	−0.09	−0.39	−0.06	0.10	0.58	−0.02	0.07
13	−0.02	0.11	−0.30	0.11	−1.12	0.09	0.08
14	−0.07	0.51	0.14	0.00	−0.61	0.10	0.00
15	0.00	−0.21	−0.21	−0.21	−0.21	−0.02	0.03
16	0.03	0.11	−0.23	0.17	−0.90	−0.07	−0.11
17	0.06	−0.39	0.09	0.26	1.04	−0.10	−0.03
18	0.11	0.48	0.08	−0.06	−0.73	0.02	−0.09
19	0.00	0.60	−0.24	−0.06	0.48	0.07	−0.06
20	−0.15	−0.13	−0.18	−0.13	−0.26	0.13	−0.13
21	−0.06	−0.73	0.29	0.00	−0.58	−0.12	0.00
22	−0.08	−0.85	0.34	0.00	−0.68	−0.14	0.04
23	0.18	−0.83	0.69	0.31	−0.83	0.08	−0.21
24	0.11	−0.76	0.17	0.51	**2.04**	−0.20	−0.06

Table X: Comparing the results of the proposed formulation with the DG allocation given in [19]

	Previous Work	Proposed Work	
	No allocation & dispatch [19]	Allocation only	Allocation & dispatch
DG bus	34, 35, 36, 37, 38	12, 16, 21, 25, 31	
DG size ratio	1:1.5:1:0.5:1	1.5:1:1:1.25:1.5	
V_n (p.u.)	1	1	optimised
P_s (kW)	23.3, 34.9 ,23.3, 11.6, 23.3	28.9, 19.3, 19.3, 24.1, 28.9	27.2, 18.1, 18.1, 22.7, 27.2
Q_s (kvar)	12.6, 18.9, 12.6, 6.3, 12.6	21.3, 11.1, 11.1, 2.2, 17.7	14.3, 9.6, 9.6, 11.9, 14.3
% Q_{s-err}	20, −59, 88, 87, −64	40, 9, 9, 82, 16	0, 0, 0, 0, 0
% Q_{s-err}^{avg}	**63.6**	**31.2**	**0**
P_{loss} (kW)	**3.31 (2.84%)**	**1.17 (0.97%)**	**0.87 (0.77%)**
V_i^{min} (p.u.)	0.946	0.987	0.961
V_i^{max} (p.u.)	1.001	1.003	0.983

uration has been utilised to improve performance further. Extensive case studies have been performed to validate the correctness and accuracy of the proposed optimal allocation. It is further validated by a day−ahead optimal dispatch of DGs and reconfiguration switches.

APPENDIX

The product terms appearing in (48) and (49) have been linearised using the process followed in [33], [36], [43]: V_i^{re} and V_i^{im} have been discretized using smaller intervals. Fig. 8 depicts the discretization of V_i^{re} using a binary variable $v_{i.k}^{re}$. The logic is formulated as follows:

$$V_{min}^{re} + b_{v.re}\sum_{k=1}^{K} v_{i.k}^{re} \leq V_i^{re} \leq V_{min}^{re} + b_{v.re}\left(1 + \sum_{k=1}^{K} v_{i.k}^{re}\right)$$

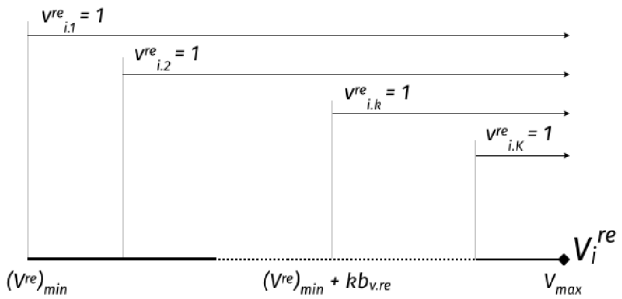


Fig. 8: Discretizing V_i^{re}

The variable $b_{v.re}$ specifies the interval size used for V_i^{re} approximation and is defined as follows:

$$b_{v.re} = \frac{V_{max} - V_{min}^{re}}{K+1}$$

where K is the number of intervals used for the approximation. For higher accuracy, the width $b_{v.re}$ should be kept as low as possible (by selecting as high as possible value for K). However, a too high value of K will lead to greater computational complexity and burden.

Now, the binary variable $v_{i.k}^{re}$ is enforced to satisfy the following condition:

$$v_{i.k}^{re} \leq v_{i.(k-1)}^{re}$$

Thus, all the voltage values falling into a particular interval is being approximated using the mid-point of that interval. Thus, the product $V_i^{re}I_{s.i}^{re}$ is approximated using the following expressions:

$$V_i^{re}I_{s.i}^{re} \approx \left(V_{min}^{re} + \frac{b_{v.re}}{2}\right)I_{s.i}^{re} + \sum_{k=1}^{K} C_{i.k}^{a}$$

where $C_{i.k}^{a}$ is a correction factor bounded as follows:

$$0 \leq b_{v.re}I_{s.i}^{re} - C_{i,k}^{a} \leq b_{v.re}\frac{P_{max}}{1.5\ V_{min}}(1 - v_{i.k}^{re})$$

$$0 \leq C_{i.k}^{a} \leq b_{v.re}\frac{P_{max}}{1.5\ V_{min}}v_{i.k}^{re}$$

The above two constraints ensure that if the value of $v_{i.k}^{re}$ is one, then $C_{i.k}^{a}$ becomes equal to $b_{v.re}I_{s.i}^{re}$, else it becomes equal to zero. In this way, the product $V_i^{re}I_{s.i}^{re}$ can be approximated by using linear terms.

Going ahead, the product $V_i^{re}I_{s.i}^{im}$ is also approximated on the similar lines using the following four equations:

$$V_i^{re}I_{s.i}^{im} \approx \left(V_{min}^{re} + \frac{b_{v.re}}{2}\right)I_{s.i}^{im} + \sum_{k=1}^{K} C_{i.k}^{b}$$

$$C_{i.k}^{b} \leq b_{v.re}I_{s.i}^{im} - b_{v.re}\frac{Q_{min}}{1.5\ V_{min}}(1 - v_{i.k}^{re})$$

$$C_{i.k}^{b} \geq b_{v.re}I_{s.i}^{im} - b_{v.re}\frac{Q_{max}}{1.5\ V_{min}}(1 - v_{i.k}^{re})$$

1949-3053 (c) 2020 IEEE. Personal use is permitted, but republication/redistribution requires IEEE permission. See http://www.ieee.org/publications_standards/publications/rights/index.html for more information.
Authorized licensed use limited to: Imperial College London. Downloaded on August 29,2020 at 19:16:47 UTC from IEEE Xplore. Restrictions apply.

This article has been accepted for publication in a future issue of this journal, but has not been fully edited. Content may change prior to final publication. Citation information: DOI 10.1109/TSG.2020.3017952, IEEE Transactions on Smart Grid

$$b_{v.re}\frac{Q_{min}}{1.5\ V_{min}}v_{i.k}^{re} \leq C_{i.k}^{b} \leq b_{v.re}\frac{Q_{max}}{1.5\ V_{min}}v_{i.k}^{re}$$

With this, the linear approximation of both the product terms involving V_i^{re} is accomplished. The product terms involving V_i^{im} has been linearised using the same process as followed for V_i^{re}. These equations have been excluded for brevity.

ACKNOWLEDGEMENT

Authors would like to acknowledge the support received from the Department of Science and Technology (DST), Ministry of Science and Technology, India under the Indo-UK project IUCERCE (India-UK Centre for Education and Research in Clean Energy, project code:16DST050).

REFERENCES

[1] X. Xu, Z. Yan, M. Shahidehpour, S. Chen, H. Wang, Z. Li, and Q. Zhou, "Maximum loadability of islanded microgrids with renewable energy generation," *IEEE Trans. Smart Grid*, vol. 10, no. 5, pp. 4696–4705, Sep. 2019.

[2] A. Milczarek, M. Malinowski, and J. M. Guerrero, "Reactive power management in islanded microgrid—proportional power sharing in hierarchical droop control," *IEEE Trans. Smart Grid*, vol. 6, no. 4, pp. 1631–1638, July 2015.

[3] H. Han, X. Hou, J. Yang, J. Wu, M. Su, and J. M. Guerrero, "Review of power sharing control strategies for islanding operation of ac microgrids," *IEEE Trans. Smart Grid*, vol. 7, no. 1, pp. 200–215, Jan 2016.

[4] M. Kosari and S. H. Hosseinian, "Decentralized reactive power sharing and frequency restoration in islanded microgrid," *IEEE Trans. Power Systems*, vol. 32, no. 4, pp. 2901–2912, July 2017.

[5] Y. Gupta, K. Chatterjee, and S. Doolla, "A simple control scheme for improving reactive power sharing in islanded microgrid," *IEEE Trans. Power Syst.*, vol. 35, no. 4, pp. 3158–3169, 2020.

[6] D. K. Dheer, Y. Gupta, and S. Doolla, "A self-adjusting droop control strategy to improve reactive power sharing in islanded microgrid," *IEEE Trans. Sustainable Energy*, vol. 11, no. 3, pp. 1624–1635, 2020.

[7] H. Mahmood, D. Michaelson, and J. Jiang, "Reactive power sharing in islanded microgrids using adaptive voltage droop control," *IEEE Trans. Smart Grid*, vol. 6, no. 6, pp. 3052–3060, Nov. 2015.

[8] M. Zhang, B. Song, and J. Wang, "Circulating current control strategy based on equivalent feeder for parallel inverters in islanded microgrid," *IEEE Trans. Power Systems*, vol. 34, no. 1, pp. 595–605, 2019.

[9] M. Eskandari, L. Li, and M. H. Moradi, "Decentralized optimal servo control system for implementing instantaneous reactive power sharing in microgrids," *IEEE Trans. Sustainable Energy*, vol. 9, no. 2, pp. 525–537, April 2018.

[10] H. Xu, X. Zhang, F. Liu, R. Shi, C. Yu, and R. Cao, "A reactive power sharing strategy of vsg based on virtual capacitor algorithm," *IEEE Trans. Industrial Electronics*, vol. 64, no. 9, pp. 7520–7531, Sept 2017.

[11] J. Zhou, S. Kim, H. Zhang, Q. Sun, and R. Han, "Consensus-based distributed control for accurate reactive, harmonic, and imbalance power sharing in microgrids," *IEEE Trans. Smart Grid*, vol. 9, no. 4, pp. 2453–2467, July 2018.

[12] R. Han, L. Meng, G. Ferrari-Trecate, E. A. A. Coelho, J. C. Vasquez, and J. M. Guerrero, "Containment and consensus-based distributed coordination control to achieve bounded voltage and precise reactive power sharing in islanded ac microgrids," *IEEE Trans. Industry Applications*, vol. 53, no. 6, pp. 5187–5199, Nov 2017.

[13] X. Lu, X. Yu, J. Lai, Y. Wang, and J. M. Guerrero, "A novel distributed secondary coordination control approach for islanded microgrids," *IEEE Trans. Smart Grid*, vol. 9, no. 4, pp. 2726–2740, 2018.

[14] J. He, Y. W. Li, and F. Blaabjerg, "An enhanced islanding microgrid reactive power, imbalance power, and harmonic power sharing scheme," *IEEE Trans. Power Electronics*, vol. 30, no. 6, pp. 3389–3401, June 2015.

[15] J. W. Simpson-Porco, Q. Shafiee, F. Dörfler, J. C. Vasquez, J. M. Guerrero, and F. Bullo, "Secondary frequency and voltage control of islanded microgrids via distributed averaging," *IEEE Trans. Ind. Electron.*, vol. 62, no. 11, pp. 7025–7038, 2015.

[16] X. Wu, C. Shen, and R. Iravani, "Feasible range and optimal value of the virtual impedance for droop-based control of microgrids," *IEEE Trans. Smart Grid*, vol. 8, no. 3, pp. 1242–1251, May 2017.

[17] J. A. Mueller and J. W. Kimball, "An efficient method of determining operating points of droop-controlled microgrids," *IEEE Trans. Energy Conversion*, vol. 32, no. 4, pp. 1432–1446, Dec 2017.

[18] A. Elrayyah, Y. Sozer, and M. E. Elbuluk, "A novel load-flow analysis for stable and optimized microgrid operation," *IEEE Trans. Power Delivery*, vol. 29, no. 4, pp. 1709–1717, Aug 2014.

[19] Y. Zhu, Q. Fan, B. Liu, and T. Wang, "An enhanced virtual impedance optimization method for reactive power sharing in microgrids," *IEEE Trans. Power Electronics*, vol. 33, no. 12, pp. 10 390–10 402, Dec 2018.

[20] X. Yang, Y. Du, J. Su, L. Chang, Y. Shi, and J. Lai, "An optimal secondary voltage control strategy for an islanded multibus microgrid," *IEEE Journal Emerging Selected Topics in Power Electronics*, vol. 4, no. 4, pp. 1236–1246, Dec 2016.

[21] A. Elrayyah, F. Cingoz, and Y. Sozer, "Construction of nonlinear droop relations to optimize islanded microgrid operation," *IEEE Trans. Industry Applications*, vol. 51, no. 4, pp. 3404–3413, July 2015.

[22] Y. Khayat, Q. Shafiee, R. Heydari, M. Naderi, T. Dragičević, J. W. Simpson-Porco, F. Dörfler, M. Fathi, F. Blaabjerg, J. M. Guerrero, and H. Bevrani, "On the secondary control architectures of ac microgrids: An overview," *IEEE Trans. Power Electron.*, vol. 35, no. 6, pp. 6482–6500, 2020.

[23] P. S. Georgilakis and N. D. Hatziargyriou, "Optimal distributed generation placement in power distribution networks: Models, methods, and future research," *IEEE Trans. Power Systems*, vol. 28, no. 3, pp. 3420–3428, Aug 2013.

[24] H. Xing and X. Sun, "Distributed generation locating and sizing in active distribution network considering network reconfiguration," *IEEE Access*, vol. 5, pp. 14 768–14 774, 2017.

[25] M. Zhang, M. Gan, and L. Li, "Sizing and siting of distributed generators and energy storage in a microgrid considering plug-in electric vehicles," *Energies*, vol. 12, no. 12, p. 2293, 2019.

[26] R. S. Rao, K. Ravindra, K. Satish, and S. V. L. Narasimham, "Power loss minimization in distribution system using network reconfiguration in the presence of distributed generation," *IEEE Trans. Power Systems*, vol. 28, no. 1, pp. 317–325, Feb 2013.

[27] M. Gheydi, A. Nouri, and N. Ghadimi, "Planning in microgrids with conservation of voltage reduction," *IEEE Systems Journal*, vol. 12, no. 3, pp. 2782–2790, Sep. 2018.

[28] S. M. Hakimi, A. Hasankhani, M. Shafie-khah, and J. P. S. Catalão, "Optimal sizing and siting of smart microgrid components under high renewables penetration considering demand response," *IET Renewable Power Generation*, vol. 13, no. 10, pp. 1809–1822, 2019.

[29] V. B. Foroutan, M. H. Moradi, and M. Abedini, "Optimal operation of autonomous microgrid including wind turbines," *Renewable Energy*, vol. 99, pp. 315 – 324, 2016.

[30] M. M. A. Abdelaziz, H. E. Farag, and E. F. El-Saadany, "Optimum reconfiguration of droop-controlled islanded microgrids," *IEEE Trans. Power Systems*, vol. 31, no. 3, pp. 2144–2153, May 2016.

[31] D. Manna, S. K. Goswami, and P. K. Chattopadhyay, "Optimisation of droop coefficients of multiple distributed generators in a microgrid," *IET Generation, Transmission Distribution*, vol. 12, no. 18, pp. 4108–4116, 2018.

[32] A. Kavousi-Fard, A. Zare, and A. Khodaei, "Effective dynamic scheduling of reconfigurable microgrids," *IEEE Trans. Power Systems*, vol. 33, no. 5, pp. 5519–5530, Sep. 2018.

[33] J. F. Franco, M. J. Rider, M. Lavorato, and R. Romero, "A mixed-integer lp model for the reconfiguration of radial electric distribution systems considering distributed generation," *Electric Power Systems Research*, vol. 97, pp. 51 – 60, 2013.

[34] J. Rocabert, A. Luna, F. Blaabjerg, and P. Rodríguez, "Control of power converters in ac microgrids," *IEEE Trans. Power Electronics*, vol. 27, no. 11, pp. 4734–4749, Nov. 2012.

1949-3053 (c) 2020 IEEE. Personal use is permitted, but republication/redistribution requires IEEE permission. See http://www.ieee.org/publications_standards/publications/rights/index.html for more information.
Authorized licensed use limited to: Imperial College London. Downloaded on August 29,2020 at 19:16:47 UTC from IEEE Xplore. Restrictions apply.

This article has been accepted for publication in a future issue of this journal, but has not been fully edited. Content may change prior to final publication. Citation information: DOI 10.1109/TSG.2020.3017952, IEEE Transactions on Smart Grid

[35] A. Arif, Z. Wang, J. Wang, B. Mather, H. Bashualdo, and D. Zhao, "Load modeling—a review," *IEEE Trans. Smart Grid*, vol. 9, no. 6, pp. 5986–5999, Nov 2018.
[36] J. F. Franco, M. J. Rider, and R. Romero, "A mixed-integer linear programming model for the electric vehicle charging coordination problem in unbalanced electrical distribution systems," *IEEE Trans. Smart Grid*, vol. 6, no. 5, pp. 2200–2210, 2015.
[37] M. M. A. Abdelaziz, "Effect of detailed reactive power limit modeling on islanded microgrid power flow analysis," *IEEE Trans. Power Systems*, vol. 31, no. 2, pp. 1665–1666, March 2016.
[38] S.-E. Razavi, E. Rahimi, M. S. Javadi, A. E. Nezhad, M. Lotfi, M. Shafie-khah, and J. P. Catalão, "Impact of distributed generation on protection and voltage regulation of distribution systems: A review," *Renewable and Sustainable Energy Reviews*, vol. 105, pp. 157 – 167, 2019.
[39] D. K. Dheer, O. V. Kulkarni, S. Doolla, and A. K. Rathore, "Effect of reconfiguration and meshed networks on the small-signal stability margin of droop-based islanded microgrids," *IEEE Trans. Industry Applications*, vol. 54, no. 3, pp. 2821–2833, May 2018.
[40] M. Lavorato, J. F. Franco, M. J. Rider, and R. Romero, "Imposing radiality constraints in distribution system optimization problems," *IEEE Trans. Power Systems*, vol. 27, no. 1, pp. 172–180, 2012.
[41] M. V. Kirthiga, S. A. Daniel, and S. Gurunathan, "A methodology for transforming an existing distribution network into a sustainable autonomous micro-grid," *IEEE Trans. Sustainable Energy*, vol. 4, no. 1, pp. 31–41, Jan 2013.
[42] M. H. Hemmatpour, M. Mohammadian, and A. A. Gharaveisi, "Optimum islanded microgrid reconfiguration based on maximization of system loadability and minimization of power losses," *Intl. Jour. of Elect. Power & Energy Syst.*, vol. 78, pp. 343 – 355, 2016.
[43] M. Resener, S. Haffner, L. A. Pereira, and P. M. Pardalos, "Mixed-integer lp model for volt/var control and energy losses minimization in distribution systems," *Electric Power Systems Research*, vol. 140, pp. 895 – 905, 2016.
[44] M. E. Baran and F. F. Wu, "Network reconfiguration in distribution systems for loss reduction and load balancing," *IEEE Trans. Power Delivery*, vol. 4, no. 2, pp. 1401–1407, April 1989.
[45] A. Maulik and D. Das, "Optimal operation of droop-controlled islanded microgrids," *IEEE Trans. Sustainable Energy*, vol. 9, no. 3, pp. 1337–1348, July 2018.
[46] A. Bokhari, A. Alkan, R. Dogan, M. Diaz-Aguiló, F. de León, D. Czarkowski, Z. Zabar, L. Birenbaum, A. Noel, and R. E. Uosef, "Experimental determination of the zip coefficients for modern residential, commercial, and industrial loads," *IEEE Trans. Power Delivery*, vol. 29, no. 3, pp. 1372–1381, June 2014.



Yusuf Gupta (S'16) was born in Mumbai, India in 1986. He received the B.Tech. degree in Electrical Engineering from Veermata Jijabai Technological Institute (VJTI), University of Mumbai, Mumbai, India in 2008. Thereafter, he worked as an Electrical Drives System Engineer in the Metals Technologies Division of Siemens Limited, Mumbai, India for six years (2008−2014). Subsequently, he worked as a Research Assistant for a brief period at the National Centre for Photovoltaic Research and Education (NCPRE) at Indian Institute of Technology (IIT) Bombay, Mumbai, India. Currently, he is working towards the Ph.D. degree at IIT Bombay, Mumbai, India. His current research interests are control and optimisation methods for planning and operation of distributed generation, microgrids and active distribution networks.



Suryanarayana Doolla (M'07, SM'15) received the B.Tech. degree in electrical engineering from Acharya Nagarjuna University, Guntur, India in 2000, the M.Tech. degree in energy systems engineering from the Indian Institute of Technology Bombay, Mumbai, India, in 2002 and the Ph.D. degree in power systems from the Indian Institute of Technology Delhi, New Delhi, India, in 2007. Currently, he is a Professor at the Department of Energy Science and Engineering, Indian Institute of Technology Bombay, Mumbai, India. His research interests are in smart microgrids, communication protocols for power systems, grid integration of distributed energy resources and demand-side management. Dr. Doolla is an Associate Editor for Electric Power Components and Systems, the IEEE Transactions on Industry Applications, the IEEE Journal of Emerging and Selected Topics in Power Electronics and the International Transactions on Electrical Energy Systems. He is also the editorial Board Member for International Journal of Sustainable Energy (Taylor and Francis Journals), Electrical Power Components and Systems and IEEE Electrification Magazine.



Kishore Chatterjee (M'10) was born in Calcutta, India, in 1967. He received the B.E. degree from the Maulana Azad National Institute of Technology (MANIT), Bhopal, India, in 1990, the M.E. degree from the Indian Institute of Engineering Science and Technology (IIEST), Howrah, India in 1992, both in electrical engineering, and the Ph.D. degree from the Indian Institute of Technology Kanpur, Kanpur, India, in 1998. From 1997 to 1998, he was a Senior Research Associate with the Indian Institute of Technology Kanpur. Since 1998, he has been with the Department of Electrical Engineering, Indian Institute of Technology Bombay, Mumbai, India, where he is currently a Professor. He has been leading the power electronic group of the National Centre for Photovoltaic Research and Education (NCPRE) being hosted at IIT Bombay since 2009. His current research interests are power evacuation strategies from solar photovoltaic systems, modern var compensators, active power filters, utility-friendly converter topologies, and induction motor drives.



Bikash C. Pal (M'00, SM'02, F'13) received the B.E.E. (with honors) degree from Jadavpur University, Calcutta, India, M.E. degree from the Indian Institute of Science, Bangalore, India, and the Ph.D. degree from Imperial College London, London, U.K, in 1990, 1992, and 1999, respectively, all in electrical engineering. He is currently a Professor with the Department of Electrical and Electronic Engineering, Imperial College London. His current research interests include renewable energy modelling and control, state estimation, and power system dynamics. He is Vice President Publications, IEEE Power and Energy Society. He was Editor-in-Chief of IEEE Transactions on Sustainable Energy (2012-2017) and Editor-in-Chief of IET Generation, Transmission and Distribution (2005-2012), and is Fellow of IEEE for his contribution to power system stability and control.

1949-3053 (c) 2020 IEEE. Personal use is permitted, but republication/redistribution requires IEEE permission. See http://www.ieee.org/publications_standards/publications/rights/index.html for more information.
Authorized licensed use limited to: Imperial College London. Downloaded on August 29,2020 at 19:16:47 UTC from IEEE Xplore. Restrictions apply.